Radio Detection of PSR J1813−1749 in HESS J1813−178: The Most Scattered Pulsar Known

F. Camilo[1] , S. M. Ransom[2] , J. P. Halpern[3] , and D. Anish Roshi[4,5]

[1] South African Radio Astronomy Observatory, 2 Fir Street, Observatory 7925, South Africa; fernando@ska.ac.za
[2] National Radio Astronomy Observatory, 520 Edgemont Road, Charlottesville, VA 22903-2475, USA
[3] Department of Astronomy, Columbia University, 550 West 120th Street, New York, NY 10027-6601, USA
[4] Arecibo Observatory, Arecibo, PR 00612, USA
[5] University of Central Florida, Orlando, FL 32816, USA

Abstract

The 44.7 ms X-ray pulsar in the supernova remnant G12.82−0.02/HESS J1813−178 has the second highest spin-down luminosity of known pulsars in the Galaxy, with $\dot{E} = 5.6 \times 10^{37}\,\mathrm{erg\,s^{-1}}$. Using the Green Bank Telescope, we have detected radio pulsations from PSR J1813−1749 at 4.4–10.2 GHz. The pulse is highly scattered, with an exponential decay timescale τ longer than that of any other pulsar at these frequencies. A point source detected at this position by Dzib et al. in several observations with the Jansky Very Large Array can be attributed to the pulsed emission. The steep dependence of τ on observing frequency explains why all previous pulsation searches at lower frequencies failed ($\tau \approx 0.25\,\mathrm{s}$ at 2 GHz). The large dispersion measure, DM = 1087 pc cm^{-3}, indicates a distance of either 6.2 or 12 kpc according to two widely used models of the electron density distribution in the Galaxy. These disfavor a previously suggested association with a young stellar cluster at the closer distance of 4.8 kpc. The high X-ray measured column density of $\approx 10^{23}\,\mathrm{cm^{-2}}$ also supports a large distance. If $d \approx 12\,\mathrm{kpc}$, HESS J1813−178 would be one of the most luminous TeV sources in the Galaxy.

Unified Astronomy Thesaurus concepts: Rotation powered pulsars (1408); Radio pulsars (1353); Galactic radio sources (571); Supernova remnants (1667); Interstellar scattering (854); Gamma-ray sources (633)

1. Introduction

HESS J1813−178 is a bright TeV source (Aharonian et al. 2005, 2006) coincident with the young shell-type radio supernova remnant (SNR) G12.82−0.02 and the 2–10 keV X-ray source AX J1813−178 (Brogan et al. 2005). It is also detected at 20–100 keV as IGR J18135−1751 (Ubertini et al. 2005). Chandra and XMM-Newton resolved the X-ray emission into a point source and bright surrounding nebula (Funk et al. 2007; Helfand et al. 2007), evidently a pulsar and its wind nebula (PWN). In subsequent X-ray timing observations, Gotthelf & Halpern (2009) and Halpern et al. (2012) discovered the $P = 44.7$ ms pulsar, with characteristic age $\tau_c = P/2\dot{P} = 5600$ yr and spin-down luminosity $\dot{E} = 4\pi^2 I\dot{P}/P^3 = 5.6 \times 10^{37}\,\mathrm{erg\,s^{-1}}$, second in power in the Galaxy only to the Crab pulsar.

Close in projection to PSR J1813−1749 is the young stellar cluster Cl 1813−178 at a kinematic distance of 4.8 kpc, discovered by Messineo et al. (2008, 2011), who proposed this as a possible birthplace of the pulsar progenitor. However, Halpern et al. (2012) argued that the discrepant measurements of optical extinction to the cluster and X-ray absorption to the pulsar/PWN, and X-ray absorption to a neighboring source of known distance, are evidence that the distance to HESS J1813−178 is greater than that to Cl 1813−178, possibly as large as 12 kpc.

Radio pulsation searches at the Green Bank Telescope (GBT) at 1.4 GHz and 2 GHz failed to detect a radio pulsar, with period-averaged flux density limits of <0.07 mJy and <0.006 mJy, respectively (Halpern et al. 2012). Despite these non-detections, a time-variable point source at the X-ray position of PSR J1813−1749 in 4.86 GHz images from the Very Large Array (VLA) was reported by Dzib et al. (2010). The measured flux density was 0.18 ± 0.02 mJy in 2006. Additional Jansky VLA (JVLA) observations by Dzib et al. (2018) in 2012, 2017,

and 2018 continued to detect a moderately variable point source at 6 GHz and 10 GHz with flux densities of ≈0.12 mJy and ≈0.06 mJy, respectively. In addition, Dzib et al. (2018) performed another pulsar search at 1.4 GHz using the 100 m Effelsberg Telescope, obtaining an upper limit of <0.065 mJy. Since the extrapolation of the steep spectrum of the JVLA 6 and 10 GHz detections to the lower frequencies of the pulsation searches greatly exceeds the flux upper limits of those searches, it is difficult to understand the non-detection of the pulsar and the nature of the compact radio source.

We report pulsation searches using the GBT at frequencies of 4.4–10.2 GHz that finally detect a highly dispersed and scattered pulse that can be attributed to the JVLA imaged point source. In Section 2 we describe the observations, and explain the lack of detection of pulsations at lower frequencies in terms of scattering. Section 3 discusses the pulsar dispersion measure (DM) distance and its implications for the luminosity of the TeV source, the location of the scattering material, as well as other properties. Suggestions for further work on this pulsar are presented in Section 4.

2. Observations

2.1. GUPPI

On 2012 July 20 we used the GUPPI spectrometer (DuPlain et al. 2008) to sample an 800 MHz band centered at 4.8 GHz, recording data from each of 512 frequency channels every 0.163 ms. The integration lasted for 70 minutes. We used standard pulsar search techniques implemented in PRESTO (Ransom 2001), searching in DM up to 3360 pc cm^{-3}, twice the total Galactic value predicted for this line of sight by the Cordes & Lazio (2002) electron distribution model. A strong detection at a barycentric period of 44.712592(12) ms was
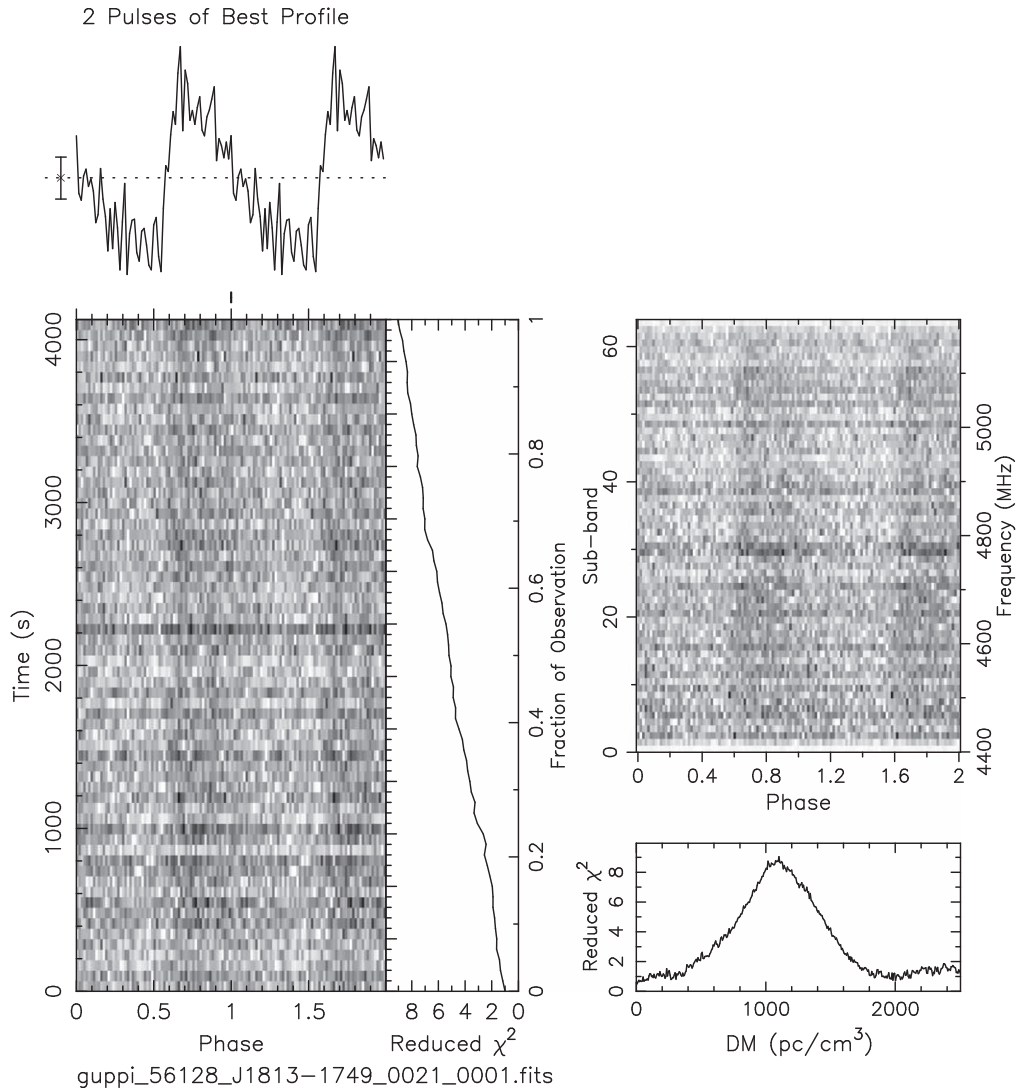
Figure 1. Radio discovery of PSR J1813−1749 on 2012 July 20 in a 70 minute GBT observation with the old C-band receiver using GUPPI (4.4–5.2 GHz). The 44 ms pulse has a clear scattering tail, which is unprecedented among pulsars at 5 GHz, and a nominal DM of 1102 pc cm^{-3}. This peak DM (based on χ^2) is biased high because of scattering at the bottom of the wide band—the best-fit DM is 1087 pc cm^{-3} (see Section 2.3). The best-fit barycentric spin period of this detection is $P = 44.71259(1)$ ms, at epoch MJD = 56128.15.

obtained, as shown in Figure 1, 2.3σ from an extrapolation of the incoherent X-ray ephemeris of PSR J1813−1749 (Halpern et al. 2012), which would predict $P = 44.712535(22)$ ms. The large DM of 1087 pc cm^{-3} implies a distance of 12 ± 2 kpc according to the Cordes & Lazio (2002) model, or 6.2 kpc in the Yao et al. (2017) model. A long, exponential scattering tail is evident even at this high frequency, making PSR J1813 −1749 clearly an extremely scattered pulsar.

We made another observation of PSR J1813−1749 on 2015 January 12, in the frequency range 5.2–6.0 GHz, this time using a new C-band receiver. The pulsar was clearly detected in the 30 minute observation (Figure 2) with a period of 44.722438(35) ms, this time with a somewhat narrower profile consistent with expectation from the typical ν^{-4} dependence of the scattering timescale on observing frequency ν. A formal measurement of the scattering timescale is made in Section 2.3. The period derivative between the two radio detections is $\dot{P} = 1.2570(37) \times 10^{-13}$, very close to the earlier X-ray measured value of $1.26545(64) \times 10^{-13}$ (Halpern et al. 2012).

2.2. VEGAS

On 2015 January 10 we also observed PSR J1813−1749 with the new Versatile GBT Astronomical Spectrometer (VEGAS) spectrometer (Prestage et al. 2015), using 0.5 ms sampling. A 60 minute observation in C-band (3.8–8.2 GHz) and a 45 minute observation in X-band (7.8–10.2 GHz) each detected the pulsar (Figures 3 and 4). The broader bandpass of VEGAS provides a higher signal-to-noise ratio (S/N) pulse profile in C-band, and a weaker pulse at X-band, with no scattering evident. These higher-quality data show that the pulse shape is complex. Rather than a single narrow pulse with an exponential tail, there appear to be two components intrinsic to the pulse profile.

A fit to all the radio and prior X-ray measured periods is shown in Figure 5, which yields an overall $\dot{P} = 1.2668(5) \times 10^{-13}$. The fit is not perfect, however, likely because of intervening glitches and/or timing noise. This $\dot{P}$ is within 3.2σ of a longer-term average value based only on X-ray measurements (Ho et al. 2020).

2 Pulses of Best Profile
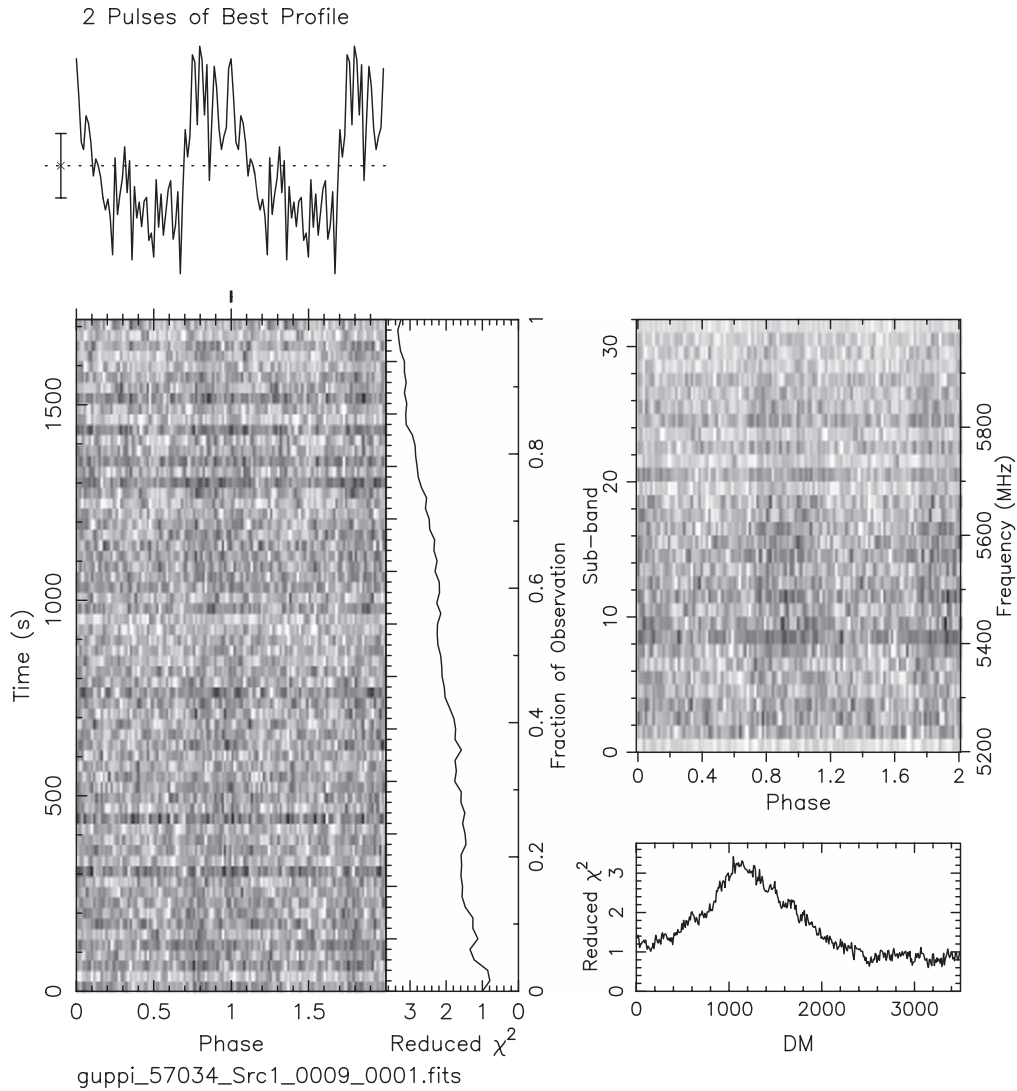

guppi_57034_Src1_0009_0001.fits

Figure 2. PSR J1813−1749 on 2015 January 12 in a 30 minute GBT observation with the new C-band receiver using GUPPI (5.2–6.0 GHz). For this detection at MJD = 57034.72, $P = 44.72244(4)$ ms.

2.3. Pulse Broadening of PSR J1813−1749

In order to estimate the amount of pulse broadening for PSR J1813−1749, we performed a simultaneous fit to the C-band and X-band VEGAS profiles (Figures 3 and 4) using the `emcee` package for Markov Chain Monte Carlo (MCMC) analyses (Foreman-Mackey et al. 2013). We assumed a simple one-sided exponential pulse broadening model, with scattering timescale $\tau(\nu)$ proportional to ν^{-4} (Oswald et al. 2021). Since we do not know the intrinsic pulse shape in these observing bands, we fitted a two-Gaussian model to the X-band data (see the top gray line in Figure 6), and assumed that this is the infinite-frequency pulse profile.

We split the C-band data into four equal subbands as a function of ν, and the X-band data into two equal subbands (black traces in Figure 6). Splitting into subbands is necessary because the timescale of scattering within the broad bands varies considerably from bottom to top as a result of the strong ν^{-4} dependence of τ. The MCMC fits included multiple nuisance parameters since the correct relative scalings between any of the six fitted profiles, the absolute alignment between the two different observations,

and the true DM of the pulsar (the measured value is slightly biased by scattering) are all unknown.

The model-dependent estimate of the pulse broadening timescale at 1 GHz is $\tau_{1\,\mathrm{GHz}} = 4.14 \pm 0.11$ s, where the quoted error is purely statistical. Systematics resulting from the low-S/N subband detections, the unknown intrinsic profile shape, and the simple scattering model could substantially modify that value. In any case, this scattering timescale (equivalent to 1.1 s at 1.4 GHz and 0.26 s at 2 GHz) would smear out almost all of the pulsed flux for this 44 ms pulsar at lower frequencies, accounting for its non-detection in pulsed searches at 1.4 GHz and 2 GHz (see Section 1). Even at 4.4 GHz (the bottom of the discovery radio band, see Figure 1), the implied 11 ms scattering timescale is 25% of the rotation period.

The MCMC-fit value of the dispersion measure is DM = 1087 ± 0.5 pc cm^{-3}, where the quoted error is purely statistical. This is model dependent (e.g., it assumes that there is no intrinsic frequency evolution of the pulse profile, and that $\tau(\nu) \propto \nu^{-4}$) and there is some covariance with other fit parameters. We estimate a systematic DM error of ≈3 pc cm^{-3}.
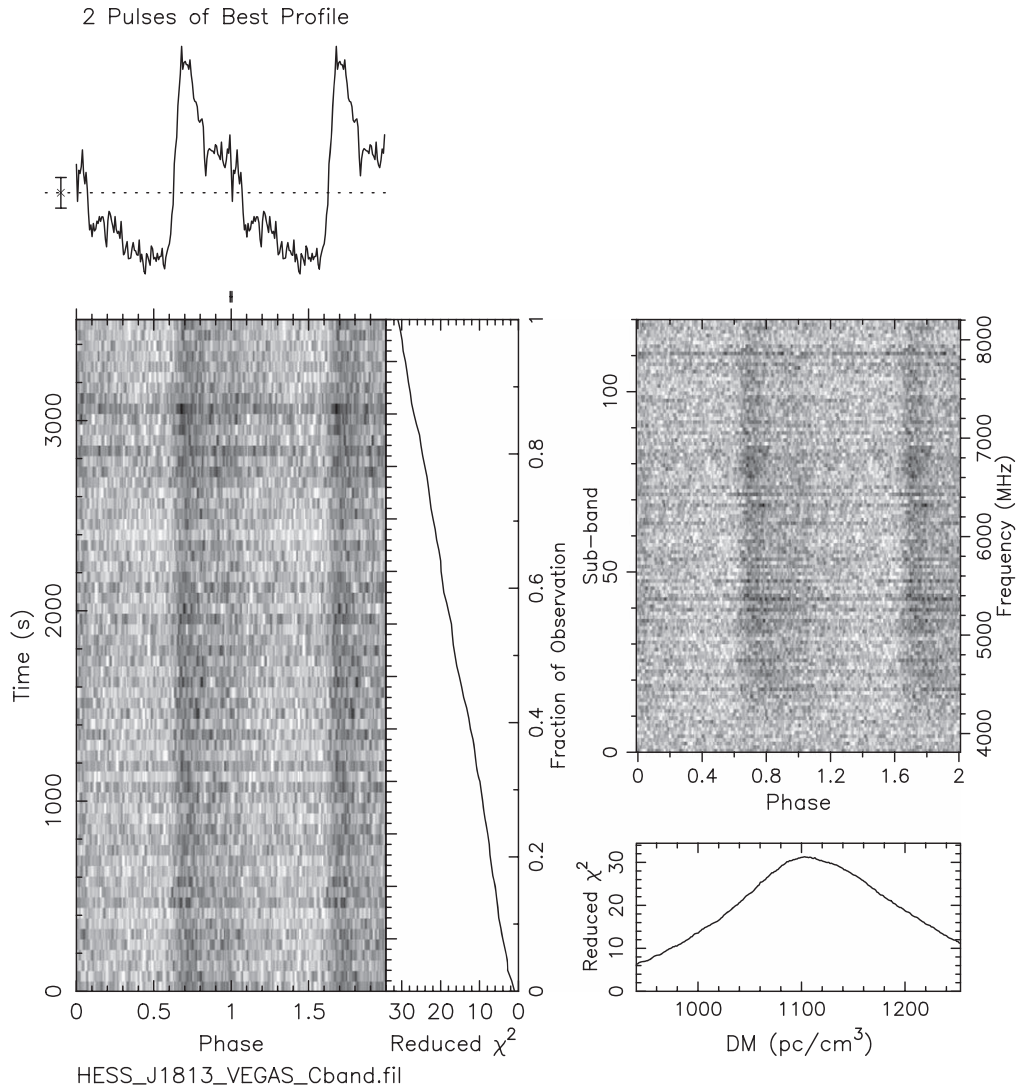
3

Figure 3. PSR J1813−1749 on 2015 January 10 in a 60 minute GBT observation with the new VEGAS spectrometer in C-band (3.8–8.2 GHz). For this detection at MJD = 57032.57, $P = 44.722434(8)$ ms.

2.4. Pulsed Flux Density of PSR J1813−1749

We obtain the period-averaged flux density S_ν for PSR J1813−1749 at C-band and X-band by applying the standard modified radiometer equation to the VEGAS detections (Section 2.2).

Prior to doing the VEGAS pulsar observations, we optimized the pointing and focusing of the subreflector/receiver system. The on-line calibration procedure for these observations returned a system temperature of 18.8 and 29.7 K for C-band and X-band, respectively. In turn, the nominal GBT gain for these bands is 1.87 and 1.8 K Jy^{-1}, respectively.

Using the above in the modified radiometer equation with parameters appropriate for the VEGAS observations (Figures 3 and 4) yields $S_{6\,\mathrm{GHz}} \approx 0.06$ mJy and $S_{9\,\mathrm{GHz}} \approx 0.06$ mJy. These are crude estimates; e.g., the C-band value may be biased low by scattering, and the X-band detection suffers from low S/N.

3. Discussion

3.1. Scattering Timescale and JVLA Point Source

PSR J1813−1749 doubtless accounts for the JVLA point source with $S_{6\,\mathrm{GHz}} \approx 0.12$ mJy and $S_{10\,\mathrm{GHz}} \approx 0.06$ mJy

(Dzib et al. 2018). First, these flux densities are comparable to those estimated from the pulsed detections (Section 2.4).

Also, despite the extreme pulse scattering, angular broadening is not expected to be detectable in the existing images. A scattering timescale τ corresponds to angular broadening of the image with FWHM

$$\theta = \sqrt{\frac{8 \ln 2\, c(d-s)\tau}{d\,s}} \qquad (1)$$

for a source at a distance d scattered by a thin screen at a distance s (Cordes & Lazio 1997). Our fitted scattering timescale at 6 GHz is $\tau_{6\,\mathrm{GHz}} = 3.2$ ms. Assuming $d = 6.2$ kpc, and $s = d/2$, the predicted angular broadening is $\theta_{6\,\mathrm{GHz}} \approx 0.''034$, which is much smaller than the typical $1.''6 \times 0.''8$ beam size of the Dzib et al. (2018) JVLA B-array observations, consistent with their detection of the pulsar as an unresolved source.

3.2. Distance, Associations, and Energetics

Arguments pertaining to the distance and possible associations with PSR J1813−1749/G12.82−0.02 were detailed by
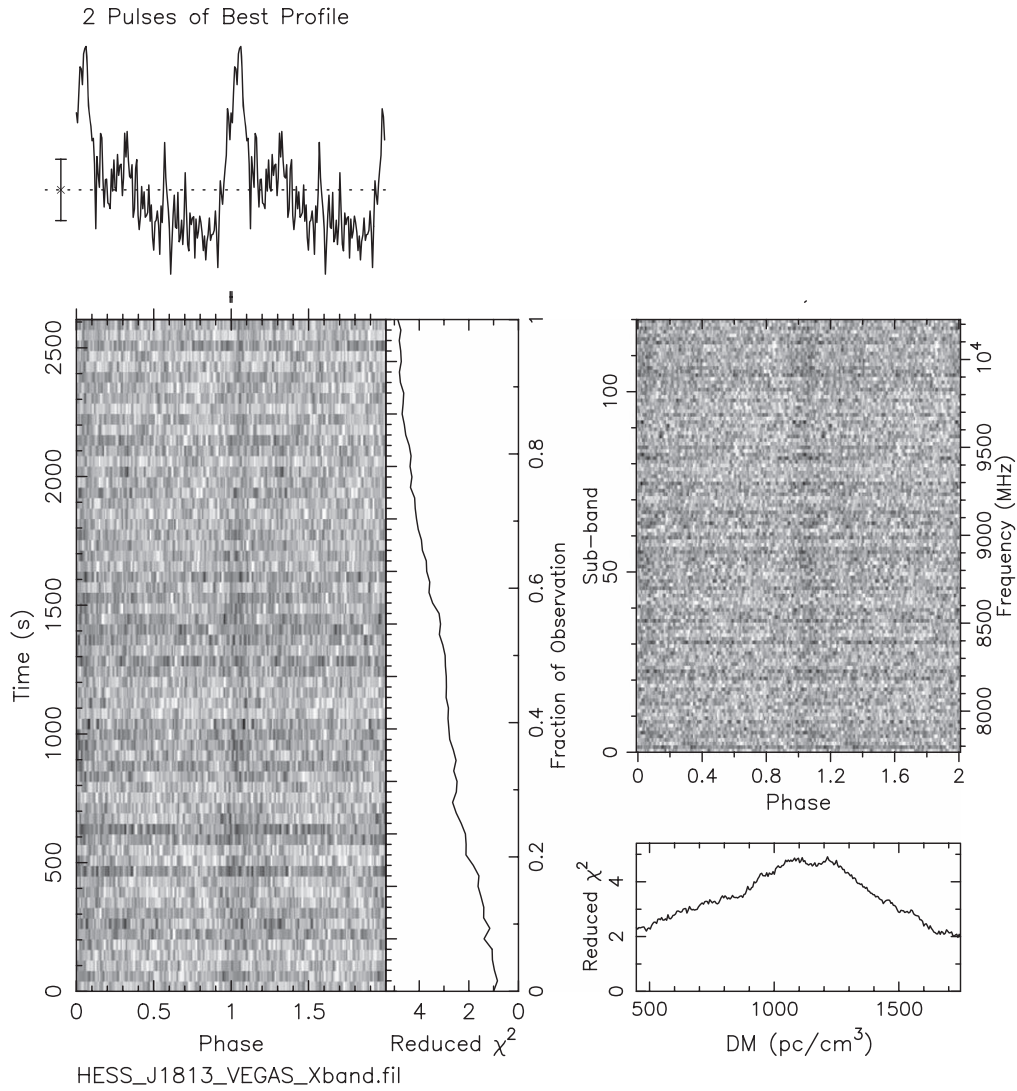
Figure 4. PSR J1813−1749 on 2015 January 10 in a 45 minute GBT observation with VEGAS in X-band (7.8–10.2 GHz). For this detection at MJD = 57032.62, $P = 44.72239(3)$ ms.

Halpern et al. (2012), and are summarized here. The young stellar cluster Cl 1813−178 is centered 4.′4 southwest of G12.82−0.02. Messineo et al. (2011) concluded that Cl 1813−178 is one of several clusters belonging to the massive star-forming region W33 at $(\ell, b) = (12°.8, -0°.2)$, and determined that it has an age of 4–4.5 Myr, which is ideal for the production of neutron stars. They derived a spectrophotometric distance to Cl 1813−178 of 3.6 ± 0.7 kpc, and a kinematic distance of 4.8 ± 0.3 kpc from the radial velocity of the brightest star in the cluster. At 4.8 kpc, the 2.′5 diameter of the SNR corresponds to a radius of 1.7 pc. Subsequent to the above work, Immer et al. (2013) measured a distance of $2.4^{+0.17}_{-0.15}$ kpc to the main W33 complexes using trigonometric parallaxes of water masers, in contradiction to a previously assumed kinematic distance of 3.7 kpc, which suggests that Cl 1813−178 is not associated with W33.

In any case, the absorbing column densities to PSR J1813−1749 and Cl 1813−178 are discrepant. The X-ray measured $N_{\rm H} = (10 \pm 1) \times 10^{22}$ cm^{-2} to G12.82−0.02 (Helfand et al. 2007) is very high. An even larger value of $N_{\rm H} = (13.1 \pm 0.9) \times 10^{22}$ cm^{-2} was derived by Ho et al. (2020) analyzing the same and

newer data. In comparison, the average visual extinction to Cl 1813−178 of $A_V = 9.1$ (Messineo et al. 2011) corresponds to an equivalent X-ray absorption of $N_{\rm H} = 2 \times 10^{22}$ cm^{-2} according to the relation $N_{\rm H} = 2.21 \times 10^{21} A_V$ cm^{-2} (Güver & Özel 2009). The highest extinction for a cluster member is $A_V = 17$ (equivalent to $N_{\rm H} = 3.8 \times 10^{22}$ cm^{-2}), which still does not come close to matching the X-ray $N_{\rm H}$. Taking into account the observed column density of molecular gas together with its velocity information from CO, it appears that the X-ray absorption is consistent with any distance in the range 5–12 kpc. The wide possible range is due to the uncertain partition of molecular gas between the near and far branches of the double-valued rotation curve. The newly measured DM is consistent with such distances as it predicts $d = 12 \pm 2$ kpc according to the Cordes & Lazio (2002) electron distribution model or 6.2 kpc in the Yao et al. (2017) model.

Further evidence for a large distance comes from a comparison with the X-ray absorption to the bright LMXB GX 13+1 that lies only 0°.7 from G12.82−0.02 along the Galactic plane. The distance to GX 13+1 was estimated as 7 ± 1 kpc (Bandyopadhyay et al. 1999) from the spectroscopic classification (K5III) of its companion star and extinction
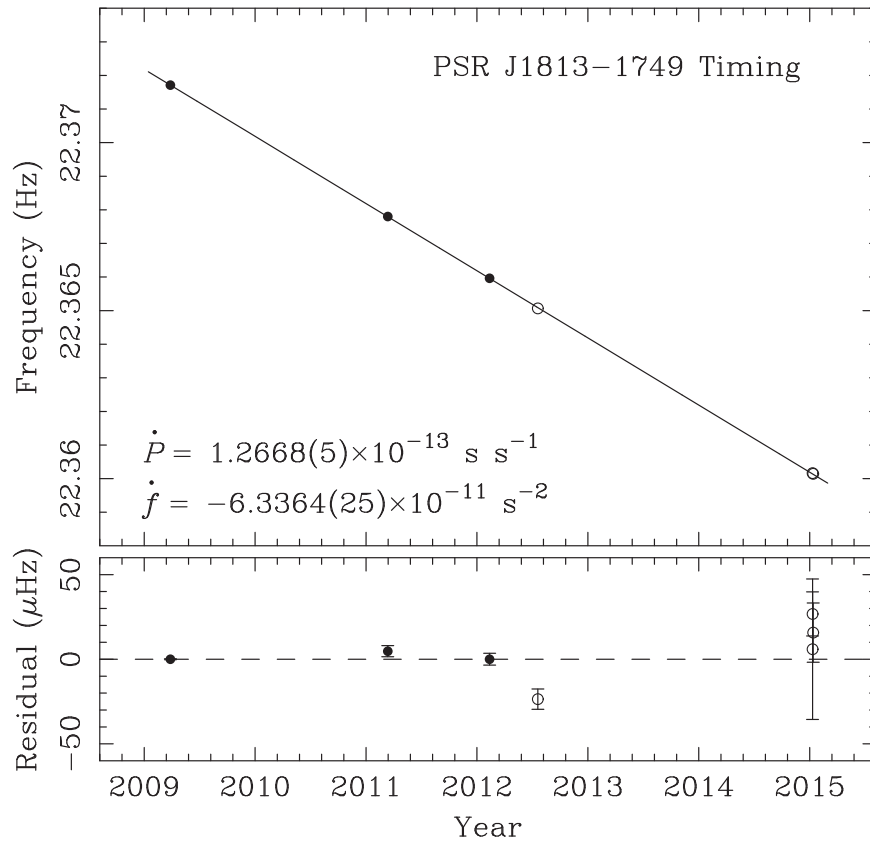
Figure 5. Timing of PSR J1813−1749. Filled circles are X-ray measurements from Halpern et al. (2012); open circles are radio measurements reported here.

variously estimated as $A_V = 13.2$–17.6, while its X-ray column density is less than one-third that to PSR J1813−1749. This suggests that the latter is farther than 7 kpc, compatible with the DM derived values. The H II regions of the intervening W33 complex may, however, contribute to the scattering of PSR J1813 −1749, similar to the conclusion of Dexter et al. (2017) concerning other pulsars and H II regions in the inner Galaxy.

If HESS J1813−178 is located at $d = 12$ kpc, its >200 GeV luminosity would be $\approx 3 \times 10^{35}$ erg s^{-1}, which is $<1\%$ of the $\dot{E}$ of PSR J1813−1749. It and HESS J1640−465 associated with PSR J1640−4631 (Gotthelf et al. 2014), also at a distance of 12 kpc, would have nearly the same luminosity and would be two of the most powerful TeV sources in the Galaxy.

3.3. Comparison with Other Pulsars

Figure 7 graphs scattering timescale against dispersion measure for the highest DM pulsars. Data are from the ATNF Pulsar Catalog[6] (Manchester et al. 2005) version 1.64, supplemented with recent measurements from MeerKAT (Oswald et al. 2021). Although there is a general correlation of $\tau_{1\text{GHz}}$ with DM among pulsars, the spread in $\tau_{1\text{ GHz}}$ at a given DM is several orders of magnitude (Löhmer et al. 2001; Lewandowski et al. 2015). This could be due to the placement of the scattering material or inadequacy of the isotropic thin-screen model. The scattering timescale of PSR J1813−1749 makes it the most scattered pulsar known, although it falls within the spread of the correlation with DM. It is not more of an outlier in

Figure 7 than, e.g., PSR J1841−0500, the intermittent pulsar discovered by Camilo et al. (2012).

The Galactic Center (GC) magnetar PSR J1745−2900 has DM $= 1778$ pc cm^{-3}, the highest of any known radio pulsar, but its scattering timescales of $\tau_{4.8\text{ GHz}} = 3.3 \pm 0.6$ ms and $\tau_{1\text{ GHz}} = 1.3$ s (Spitler et al. 2014) are smaller than those of PSR J1813 −1749. Bower et al. (2014) used the equality of the image broadening of PSR J1745−2900 and Sgr A* to argue that they are scattered by the same screen, which Equation (1) places at 2–3 kpc from Earth rather than near the GC. Such a determination of the scattering location cannot yet be made for PSR J1813 −1749 because its image size has not been measured.

What else we know from pulsars close to the line of sight is summarized in Table 1, which lists data on four pulsars at $<0°.5$ angular distance from PSR J1813−1749. All four have DM distances greater than the parallax distance of W33, but none is as distant as PSR J1813−1749. The two with the largest DM (other than PSR J1813−1749) are closest to the Galactic plane, but do not have scattering timescales measured. The two with reported scattering measurements have timescales much smaller than that of PSR J1813−1749. Together, these data argue that PSR J1813−1749 lies behind additional, distant scattering material that is not associated with the W33 complex and not traversed by the other pulsars' sightlines.

3.4. Proper Motion and Age

Recently, Ho et al. (2020) reported a proper motion of $0''.0655 \pm 0''.0114$ yr^{-1} for PSR J1813−1749 using three Chandra images over 10 yr. This implies a high tangential velocity of $v_t = 1490$ km s^{-1} at the 4.8 kpc distance assumed in

---

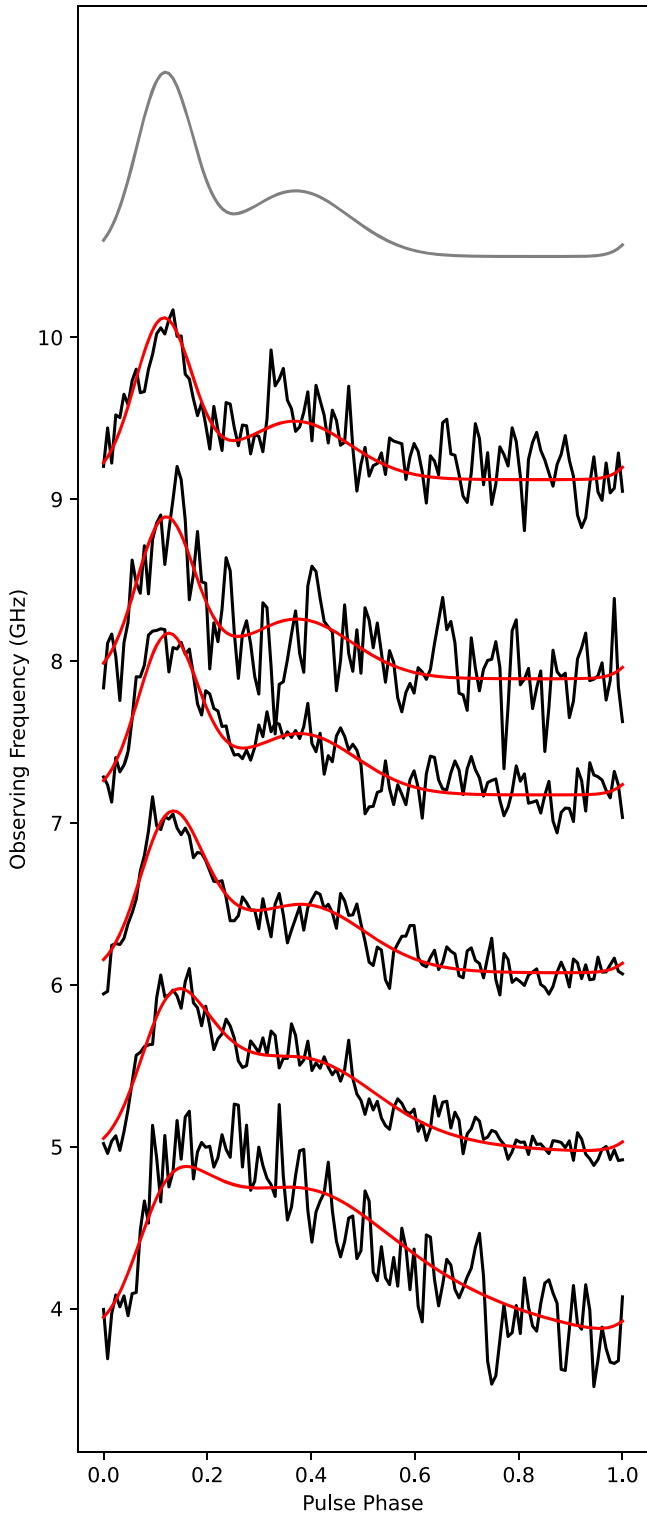[6] https://www.atnf.csiro.au/research/pulsar/psrcat/

Figure 6. Scattering fit to PSR J1813−1749 profiles at C- and X-bands. The lower four black traces are the observed profiles in four C-band subbands (see Figure 3), and the upper two black traces are two X-band subband profiles (see Figure 4). The gray trace is the assumed infinite-frequency intrinsic pulse profile based on a fit to the X-band data (Figure 4). The red traces are model profile fits of the six subbands (see Section 2.3 for details).

previous studies, but an even larger $v_t = 1925 \, \mathrm{km \, s^{-1}}$ if it is at the Yao et al. (2017) distance of 6.2 kpc. This would be larger than any well-measured velocity for a neutron star

(see Deller et al. 2019), a result that invites skepticism as well as exploration of its implications.

For one, PSR J1813−1749 is only ≈20″ from the center of the radio shell of G12.82−0.02, unlike other high-velocity pulsars that have either escaped their shells or show other morphological evidence of high velocity in the structure of their PWNe (for a review, see Kargaltsev et al. 2017). These properties might, however, be reconciled if G12.82−0.02 has a very young age of ≈300 yr. This would possibly make PSR J1813−1749 the youngest known neutron star in the Galaxy. If so, it would also be interesting if such a young SNR is accompanied by dense plasma that could cause the extreme scattering of the radio pulses. Note from Equation (1) that for a scattering screen very close to the pulsar ($s \approx d$), a given image broadening would correspond to a very large scattering timescale τ.

On the other hand, countervailing evidence against such a young age is found in the broadband spectral energy distribution of HESS J1813−178, which is more like those of evolved SNRs, and has been modeled most recently with an age of 2500 yr (Zhu et al. 2018). In summary, there would be obstacles to attributing the scattering of PSR J1813−1749 to a very young age.

4. Conclusions and Suggestions for Further Work

Pulsation searches at high radio frequency were necessary to overcome the extremely long scattering timescale of PSR J1813 −1749, the largest among known pulsars. The GBT pulsed radio detection at 4.4–10.2 GHz with DM = 1087 pc cm^{-3} provides additional evidence of a larger distance than once assumed, now favoring $d \approx 6$–14 kpc. If at the higher end of this range, HESS J1813−178 may be one of the most luminous TeV source in the Galaxy, at the expense of <1% of the spin-down power of PSR J1813−1749. A complete census of pulsars in the Galaxy, even energetic ones such as PSR J1813 −1749, remains a challenging prospect if there are more lines of sight with such long scattering timescales.

Previous modeling of the spectral energy distribution of HESS J1813−178 as leptonic emission from an evolving PWN in an expanding SNR (Fang & Zhang 2010; Zhu et al. 2018) used a distance of 4.7 kpc. Models should also be recalculated for the now favored larger distances. However, it is not universally accepted that the PWN is the source of the TeV emission, as opposed to the SNR shell or hadronic interactions with the environment (Torres et al. 2014).

Since the DM distance still has a large uncertainty, it would be worthwhile to obtain a more sensitive observation of 21 cm H I absorption against G12.82−0.02 to pin down a kinematic distance. Future Chandra observations are needed to confirm or disprove the reported high proper motion of PSR J1813−1749, which would imply a very young age for the system, and possibly be related to the extreme pulse scattering timescale. VLBI at 5 GHz could also measure proper motion, as well as image broadening that could be used to deduce the location of the scattering medium.

Finally, the detection in Figure 3 indicates that the combination of C-band and VEGAS can produce high-S/N pulse profiles in only a few minutes of observing time, opening opportunities to obtain a phase-connected timing solution for PSR J1813−1749. This might lead to the determination of its spin-down braking index, which is an important parameter to model the broadband (spectral) evolution and energetics of its PWN and HESS J1813−178.
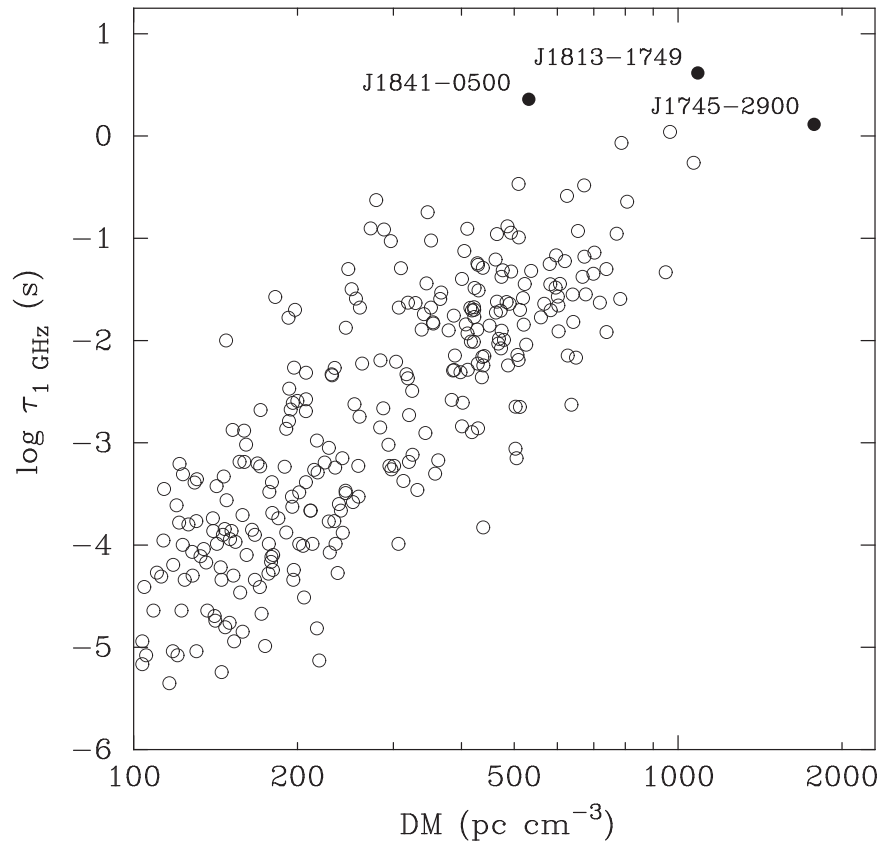
Figure 7. Scattering timescale at 1 GHz vs. dispersion measure for pulsars with the highest DM. Open circles are from the ATNF Pulsar Catalog (Manchester et al. 2005), supplemented with recent measurements from MeerKAT (Oswald et al. 2021). Labeled pulsars (filled circles) are discussed in Section 3.3.

Table 1
Pulsars within $0°5$ of PSR J1813−1749

Name (PSR)	ℓ (°)	b (°)	DM[a] (pc cm^{-3})	d[b] (kpc)	$\tau_{1\,GHz}$[a] (s)	θ (°)
J1811−1736	12.82	0.43	473.93(4)	4.4	0.042(1)	0.45
J1812−1733	12.90	0.38	509.8(1)	4.5	0.102(1)	0.41
J1813−1749	12.81	−0.02	1087(3)	6.2	4.14(11)	⋯
J1814−1744	13.02	−0.21	792(16)	5.0	⋯	0.28
J1815−1738	13.17	−0.27	724.6(2)	4.9	⋯	0.44

Notes.
[a] Uncertainties on the last digits are in parentheses.
[b] DM distance from the Yao et al. (2017) model.

ORCID iDs

F. Camilo ⓘ https://orcid.org/0000-0002-1873-3718
S. M. Ransom ⓘ https://orcid.org/0000-0001-5799-9714
J. P. Halpern ⓘ https://orcid.org/0000-0003-4814-2377
D. Anish Roshi ⓘ https://orcid.org/0000-0002-1732-5990

References

Aharonian, F., Akhperjanian, A. G., Aye, K.-M., et al. 2005, Sci, 307, 1938
Aharonian, F., Akhperjanian, A. G., Bazer-Bachi, A. R., et al. 2006, ApJ, 636, 777
Bandyopadhyay, R. M., Shahbaz, T., Charles, P. A., & Naylor, T. 1999, MNRAS, 306, 417
Bower, G. C., Deller, A., Demorest, P., et al. 2014, ApJL, 780, L2
Brogan, C. L., Gaensler, B. M., Gelfand, J. D., et al. 2005, ApJL, 629, L105
Camilo, F., Ransom, S. M., Chatterjee, S., Johnston, S., & Demorest, P. 2012, ApJ, 746, 63
Cordes, J. M., & Lazio, T. J. W. 1997, ApJ, 475, 557
Cordes, J. M., & Lazio, T. J. W. 2002, arXiv:astro-ph/0207156
Deller, A. T., Goss, W. M., Brisken, W. F., et al. 2019, ApJ, 875, 100
Dexter, J., Deller, A., Bower, G. C., et al. 2017, MNRAS, 471, 3563
DuPlain, R., Ransom, S., Demorest, P., et al. 2008, Proc. SPIE, 7019, 70191D
Dzib, S., Rodríguez, L. F., Karupussamy, R., Loinard, L., & Medina, S.-N. X. 2018, ApJ, 866, 100
Dzib, S., Rodríguez, L. F., & Loinard, L. 2010, RMxAA, 46, 153
Fang, J., & Zhang, L. 2010, ApJ, 718, 467
Foreman-Mackey, D., Hogg, D. W., Lang, D., & Goodman, J. 2013, PASP, 125, 306
Funk, S., Hinton, J. A., Moriguchi, Y., et al. 2007, A&A, 470, 249
Gotthelf, E. V., & Halpern, J. P. 2009, ApJL, 700, L158
Gotthelf, E. V., Tomsick, J. A., Halpern, J. P., et al. 2014, ApJ, 788, 155
Güver, T., & Özel, F. 2009, MNRAS, 400, 2050
Halpern, J. P., Gotthelf, E. V., & Camilo, F. 2012, ApJL, 753, L14
Helfand, D. J., Gotthelf, E. V., Halpern, J. P., et al. 2007, ApJ, 665, 1297
Ho, W. C. G., Guillot, S., Saz Parkinson, P. M., et al. 2020, MNRAS, 498, 4396
Immer, K., Reid, M., Menten, K. M., Brunthaler, A., & Dame, T. M. 2013, A&A, 553, A117

Kargaltsev, O., Pavlov, G. G., Klinger, N., & Rangleov, B. 2017, JPIPh, 83, 635830501
Lewandowski, W., Kowalińska, M., & Kijak, K. 2015, MNRAS, 449, 1570
Löhmer, O., Kramer, M., Mitra, D., Lorimer, L., & Lyne, A. G. 2001, ApJL, 562, L157
Manchester, R. N., Hobbs, G. B., Teoh, A., & Hobbs, M. 2005, AJ, 129, 1993
Messineo, M., Davies, B., Figer, D. F., et al. 2011, ApJ, 733, 41
Messineo, M., Figer, D. F., Davies, B., et al. 2008, ApJL, 683, L155

Oswald, L. S., Karastergiou, A., Posselt, B., et al. 2021, MNRAS, 504, 1115
Prestage, R. M., Bloss, M., Brandt, J., et al. 2015, in USNC-URSI Radio Science Meeting (Piscataway, NJ: IEEE), 4
Ransom, S. M. 2001, PhD thesis, Harvard Univ.
Spitler, L. G., Lee, K. J., Ethough, R. P., et al. 2014, ApJL, 780, L3
Torres, D., Cillis, A., Martín, J., & de Oña Wilhelmi, E. 2014, JHEAp, 1, 31
Ubertini, P., Bassani, L., Malizia, A., et al. 2005, ApJL, 629, L109
Yao, J. M., Manchester, R. N., & Wang, N. 2017, ApJ, 835, 29
Zhu, B.-T., Zhang, L., & Fang, L. 2018, A&A, 609, A110